Control of the Exciton Radiative Lifetime in van der Waals Heterostructures

H. H. Fang, B. Han, C. Robert, M. A. Semina, D. Lagarde, E. Courtade, T. Taniguchi, K. Watanabe, T. Amand, B. Urbaszek, M. M. Glazov, and X. Marie

Phys. Rev. Lett. **123**, 067401 — Published 5 August 2019

DOI: 10.1103/PhysRevLett.123.067401

Control of the Exciton Radiative Lifetime in van der Waals Heterostructures

H.H. Fang[1*], B. Han[1*], C. Robert[1], M.A. Semina[2], D. Lagarde[1], E. Courtade[1], T. Taniguchi[3], K. Watanabe[3], T. Amand[1], B. Urbaszek[1], M.M. Glazov[2], and X. Marie[1]
[1] *Université de Toulouse, INSA-CNRS-UPS, LPCNO, 135 Av. Rangueil, 31077 Toulouse, France*
[2] *Ioffe Institute, 194021 St. Petersburg, Russia and*
[3] *National Institute for Materials Science, Tsukuba, Ibaraki 305-0044, Japan*

Optical properties of atomically thin transition metal dichalcogenides are controlled by robust excitons characterized by a very large oscillator strength. Encapsulation of monolayers such as $MoSe_2$ in hexagonal boron nitride (hBN) yields narrow optical transitions approaching the homogenous exciton linewidth. We demonstrate that the exciton radiative rate in these van der Waals heterostructures can be tailored by a simple change of the hBN encapsulation layer thickness as a consequence of the Purcell effect. The time-resolved photoluminescence measurements show that the neutral exciton spontaneous emission time can be tuned by one order of magnitude depending on the thickness of the surrounding hBN layers. The inhibition of the radiative recombination can yield spontaneous emission time up to 10 ps. These results are in very good agreement with the calculated recombination rate in the weak exciton-photon coupling regime. The analysis shows that we are also able to observe a sizeable enhancement of the exciton radiative decay rate. Understanding the role of these electrodynamical effects allow us to elucidate the complex dynamics of relaxation and recombination for both neutral and charged excitons.

The control of the spontaneous emission using a cavity to tune the number of electromagnetic modes coupled to the emitter has been demonstrated in various atomic and solid-state systems, following the pioneering work of Purcell [1–6]. Remarkably, it was shown recently that ultra-thin semiconductors such as transition metal dichalcogenide (TMD) monolayers encapsulated in hexagonal boron nitride (hBN) exhibit spontaneous emission-dominated optical transition linewidths [7–9]. A very strong light matter interaction in these 2D materials has triggered a great interest both from a fundamental point of view and for possible optoelectronic applications [10–18]. In order to enhance the optical emission, the TMD monolayers have been integrated with various photonic crystal structures [19–21]. The optical properties are governed here by very robust excitons with binding energies of a few hundreds of meV and very large oscillator strength [22]. Owing to hBN induced surface protection and substrate flatness which reduce the inhomogeneous broadening [7], the exciton lines in encapsulated TMD monolayers (ML) are mainly dominated by homogeneous broadening which allow for instance the realisation of very efficient atomically thin mirrors [8, 9]. In these van der Waals heterostructures, the surrounding hBN layers change the dielectric environment for the excitons in the TMD monolayer, resulting in different binding energies and oscillator strengths [23, 24]. However its impact on the exciton radiative recombination dynamics due to modification of photon modes in these atomically flat layers has not been evidenced so far.

In this Letter we demonstrate that the top and bottom hBN encapsulation layers form a microcavity-like structure which controls the exciton radiative lifetime in the $MoSe_2$ monolayer through the Purcell effect. In this weak coupling regime, the escape time of spontaneous photons out of our open cavity-like structure is much shorter than the radiative lifetime and reabsorption is negligible. This is in contrast with the strong coupling regime obtained with much more reflective mirrors resulting in microcavity polaritons [25]. As the spontaneous emission probability is proportional to the amplitude of the electromagnetic field mode, the variation of the local density of optical modes within the cavity is at the origin of the variation of the radiative recombination rate. In time-resolved photoluminescence (PL) measurements we demonstrate that the exciton radiative lifetime in $MoSe_2$ monolayer can be tuned by about one order of magnitude as a function of the hBN thickness, in very good agreement with the calculated dependence using transfer matrix techniques [24]. Remarkably the measured variations of the radiative lifetime measured here (typically from 1 to 10 ps) are much larger than the ones reported previously in open semiconductor cavities based on dielectric mirrors [26, 27]. The tuning of the radiative lifetime demonstrated here for encapsulated $MoSe_2$ monolayers should also apply to other semiconductor 2D materials and associated heterostructures.

Samples and setup. We have investigated $MoSe_2$ MLs encapsulated in hBN deposited onto a 80 nm SiO_2/Si substrate using a dry-stamping technique [28], see Fig. 1(a) and Supplementary Information (SI [29]) for the details on the fabrication technique. This easy and versatile technique allows us to fabricate various van der Waals heterostructures where the density of optical modes at the location of the TMD monolayer is tuned. During the fabrication process the thickness for each hBN layer was accurately measured by Atomic Force Microscopy (AFM) with a typical resolution of ± 3 nm for the top hBN and ± 5 nm for the bottom hBN layer. We present the results on four samples with different bot-

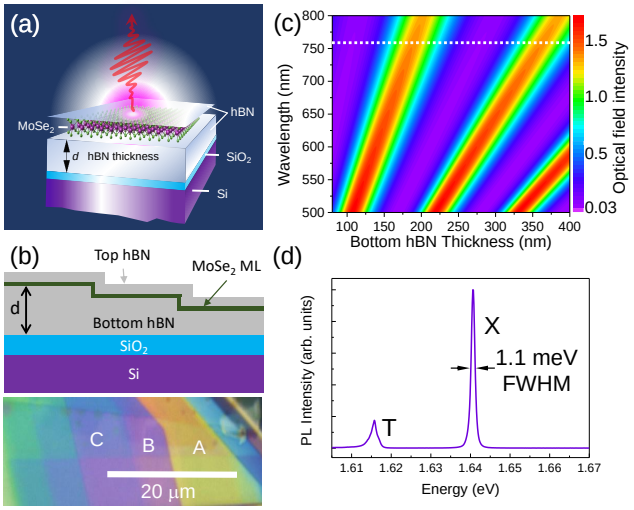

FIG. 1: (a) Schematics of the investigated $MoSe_2$ monolayer embedded in hexagonal Boron Nitride. (b) Schematics of the cross section and optical microscope image of the van der Waals heterostructure hBN/ML MoS_2/hBN (Sample III) where the same monolayer is embedded in a cavity-like structure characterized by different bottom hBN layer thickness d. (c) Optical intensity map calculated at the $MoSe_2$ monolayer location as a function of both the emission wavelength and the bottom hBN layer thickness d. The horizontal white dotted line corresponds to the neutral exciton emission wavelength ($\sim$ 756 nm). (d) *cw* photoluminescence spectrum of sample II ($d = 273$ nm) showing the emission of both the neutral (X) and charged (T) exciton, T=7 K.

tom hBN thicknesses: In samples I and II, the bottom hBN thickness is d=180 and 273 nm respectively, corresponding to the $MoSe_2$ ML located, respectively, at the anti-node and the node of the standing wave according to the calculation of the electric field distribution, Fig. 1(c). For the sample III, the same $MoSe_2$ ML is deposited on a hBN flake exhibiting different terraces and steps with hBN thicknesses $d = 206$, 237, 247 and 358 nm for zone A, B, C and D respectively, Fig. 1(b) (the terrace D is outside the optical microscope image). Sample IV is similar to sample III with two terraces $d = 125$ and $d = 149$ nm. This allows us to investigate the exciton dynamics of the same $MoSe_2$ ML and different bottom hBN layer thicknesses. The top hBN thickness does not play a key role here considering its small value of 9, 7, 8 and 8.5 nm in sample I, II, III and IV respectively.

Figure 1(b) shows an optical microscope image of the Sample III illuminated with white light from a halogen lamp. For each hBN thickness, the observed color in each zone on the sample agrees very well with the one obtained by calculating the reflectivity spectra using a transfer matrix method [24] with no adjustable parameters, using the hBN thicknesses measured by AFM and the measured hBN refractive index from Ref. [37], (see SI [29]). Figure 1(c) presents the light intensity map calculated at the ML location as a function of both the emission wavelength and the bottom hBN thickness. The Fabry-Perot interference effects and its dependence on the bottom hBN thickness are clearly seen. Continuous wave (*cw*) and time-resolved PL experiments are performed at $T = 7$ K using a He-Ne laser (633 nm) and a Ti:Sa mode-locked laser ($\sim$ 1.5 ps pulse width, 80 MHz repetition rate) respectively, see the experimental details in SI [29, 38, 39]. The typical excitation power is 5 μW and the spot diameter about 1 μm, i.e., in the linear regime of excitation which allows discarding any Auger type or stimulated emission processes [40].

Results and discussion. The encapsulation of TMD monolayers with hBN results in high optical quality samples with well-defined optical transitions exhibiting linewidth in the 1 ...4 meV range at low temperature [7, 41, 42]. Figure 1(d) displays the *cw* PL spectrum for sample II. In agreement with previous studies, both neutral exciton (X) and trion i.e., charged exciton (T) are clearly observed, with a PL linewidth of X as small as 1.1 meV (Full Width at Half Maximum, FWHM).

Figure 2 presents the key results of this investigation. In Fig. 2(a), the normalized luminescence intensity dynamics of the neutral exciton X is plotted for samples I and II (differing only by the bottom hBN thickness of 180 and 273 nm respectively). While the decay time is similar in both samples with a typical value of $\sim$ 18 ps, the PL rise time is clearly different: it is much shorter in sample I (limited by the time-resolution of the set-up), compared to a value of $\sim$ 10 ps in sample II. In general, the rise and decay rates of PL signal are determined by the interplay between the feeding rate of the radiative state and the recombination rate. In our case, the rise time of luminescence corresponds to the exciton radiative recombination time whereas the PL decay reflects the relaxation time of photogenerated excitons at higher energies towards the radiative states ($K \approx 0$). This counter-intuitive result is in part because the relaxation time, τ_{relax} , is longer than recombination time, τ_X, and can be easily modeled with a basic two-level model as shown in the inset of Fig. 3(b). The experimental results in Fig. 2(a) can be perfectly fitted by the resulting bi-exponential dynamics (see SI [29] for details): The PL decay time is not controlled by the radiative recombination time but it corresponds to the feeding time of the radiative states, see Fig. 3(b) for the fit on sample II. Taking into account the instrument response time, we find τ_{relax} =18 ps in both samples whereas $\tau_X = 11 \pm 1$ ps is typically 10 times larger in sample II compared to sample I with $\tau_X < 1.5$ ps. This is exactly the expected behaviour due to the inhibition of the spontaneous lifetime in sample II as the ML is located at the node of the electric field in the cavity-like structure (see Fig. 2(b)). Changing the excitation laser wavelength over the range 710-753

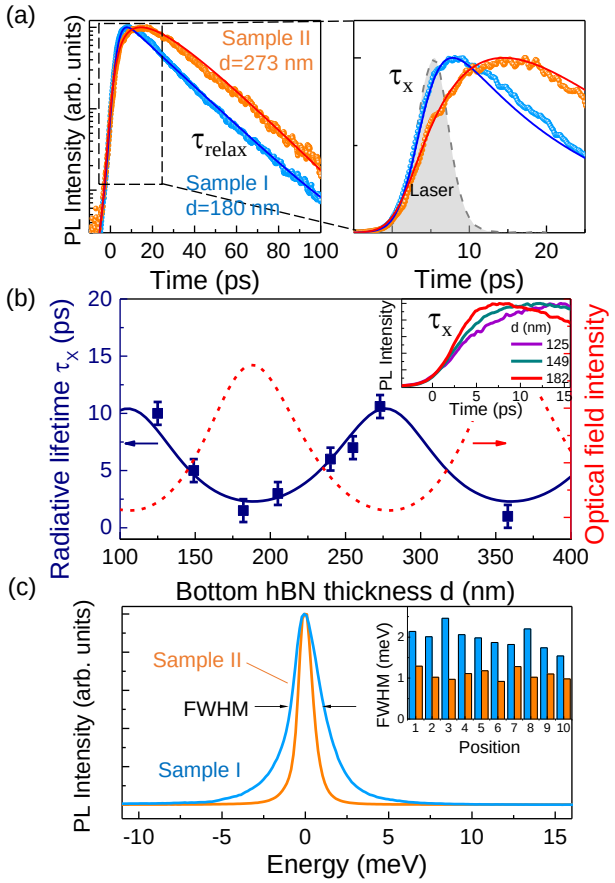

FIG. 2: (a) Left: normalized photoluminescence intensity (log scale) of the neutral exciton X as a function of time for sample I (d = 180 nm) and sample II (d = 273 nm); the full lines correspond to the bi-exponential fits (see text). The instrument response is obtained by detecting the backscattered laser pulse (wavelength 712 nm) on the sample surface, see the dotted line labeled 'Laser'; Right: zoom of the rise-time (linear scale). (b) Calculated (full line) and measured (symbols) neutral exciton radiative lifetime as a function of the hBN bottom layer thickness d. The red dashed curve is the calculated intensity of electromagnetic field in our structure (same calculation as in Fig. 1(c)) . Inset: normalized time-resolved photoluminescence intensity in sample III for three different hBN bottom layer thicknesses. (c) Normalized *cw* PL intensity of the neutral exciton in sample I and sample II clearly showing different linewidths. Because the energy of the PL peak slightly depends on the sample and sample' position by a few meV, the origin of the energy axis is taken at the PL peak. Inset: PL linewidth (FWHM) for 10 different positions in sample I and II.

nm produces non measurable variations of the exciton dynamics (see SI [29]). Note that in previous measurements of the exciton dynamics in bare TMDC monolayers the radiative recombination time was assigned to the decay of the emission signal [38, 39, 43]. This control of the radiative lifetime by the cavity effect is confirmed by the measurement of the excitonic dynamics in samples III and IV where the same $MoSe_2$ monolayer is encapsulated by hBN of different thickness. Figure 2(b) displays the exciton radiative lifetime as a function of the hBN thickness (obtained with the same fitting procedure as above). The inset of Fig. 2(b) shows the measured PL rise times in sample III for different thicknesses. We have compared the measured variation with the calculated one using the transfer matrix method (see Ref. [24] and SI [29]), extracting the exciton radiative decay rate $\Gamma_0^{\rm eff}$ from the pole of numerically calculated absorbance and using the relation [44]

$$\tau_X = \hbar/(2\Gamma_0^{\rm eff}). \quad (1)$$

Assuming a free space radiative lifetime of $MoSe_2$ ML of 2.7 ps which is the single free parameter, we find in Fig. 2(b) that the measured radiative lifetime is in very good agreement with the calculated one. Fig. 2(b) demonstrates that the exciton spontaneous lifetime can be tuned by more than one order of magnitude. This is much larger than the small variations (10-30 % typically) reported previously with Bragg reflector microcavities using III-V semiconductor quantum wells as emitters [26, 27]. Significant modulations of the radiative lifetimes due to Purcell effect were evidenced in open cavities using metallic mirrors [45] or with 3D cavity with additional lateral mode confinement: a typical factor 10 was for instance reported for quantum dots embedded in micro-pillars [5, 6]. We emphasize that the radiative lifetimes in the picosecond range evidenced in Fig. 2 are fully consistent with the recent measurements by Four-Wave Mixing (FWM) experiments of the radiative broadening in a $MoSe_2$ monolayer encapsulated in hBN [46].

A striking feature is that the cavity effect related to the hBN encapsulation has also a strong influence on the excitonic linewidth measured in *cw* PL spectroscopy. As shown in Fig. 2(c), the *cw* PL linewidth is about twice smaller in sample II ($\sim$ 1.1 meV FWHM) compared to the one in sample I ($\sim$ 2.2 meV), a trend fully consistent with the expected variation of the radiative linewidth, Eq. (1), due to the cavity effect. The linewidth usually includes both a homogeneous and inhomogeneous contribution and the latter can fluctuate in different points of a given monolayer as a result of the local dielectric disorder. Nevertheless, the average of the measurements recorded for different points on the sample II (with longer τ_X) is significantly lower than that on sample I. From the measurements on 10 different points on each sample, inset of Fig. 2(c), we find a linewidth (FWHM) of 1.1 $\pm$0.13 meV and 2.0$\pm$0.25 meV on sample II and I respectively. As expected a larger linewidth is measured in sample I characterized by a much shorter radiative lifetime, see Fig. 2(a). This result is confirmed for sample IV for different cavity lengths (see SI). As the exciton linewidth in TMDC monolayers is mainly dominated by radiative broadening [7–9, 47, 48], the control of the exciton spontaneous lifetime due to the cavity effect evidenced in Fig. 2(a) and (b) also yields a tuning of the exciton linewidth [49, 50].

However, linear techniques such as photoluminescence or reflectivity spectroscopy used here cannot disentangle the linewidth contributions from inhomogeneous broadening, non-radiative processes, light scattering and radiative decay. This would require the use of non-linear techniques such as FWM experiments [46–48]. Nevertheless, the exciton linewidth measured in sample I allows us to estimate the radiative lifetime in this sample (the time-resolved PL measurements demonstrate that it is shorter than $\sim$ 1.5 ps); from the analysis presented in the SI [29] we can infer $\tau_X \sim 740$ fs. This value is close to previous estimations where the cavity effect was not considered [8, 9, 46, 48, 51]. By comparing the measured radiative lifetime and the measured linewidth in *cw* PL, we find that the latter is not fully controlled by spontaneous emission time and inhomogeneity must still be considered. This is also consistent with recent FWM experiments [46].

Finally, the control of the radiative lifetime resulting from the hBN encapsulation is further confirmed by measuring the dynamics of the charged exciton (trion, T). Figure 3(a) displays the normalized luminescence intensity dynamics of the charged exciton T for different hBN thicknesses in sample III. In contrast to the neutral exciton the variation of the bottom hBN thickness has here an impact on the trion luminescence decay time (and not on its rise-time). As the charged exciton oscillator strength is smaller than the neutral exciton one [21, 52], the trion radiative lifetime of the order of $\sim$ 100 ps is now longer than the relaxation/formation time. As a result, the PL rise time corresponding to this energy relaxation time does not vary with the cavity thickness. Here, the striking feature is that we find a variation of the trion PL decay time as a function of the hBN thickness very similar to the variation of the neutral exciton radiative time, Fig. 2(b). Nevertheless, the amplitude of the variation is much smaller for the trion (typically 10%) whereas in the same sample the measured neutral exciton lifetime varies by more a factor two ($\sim$ 3 to 7 ps), Fig. 2(b).

The cavity effects revealed in this work make it possible to elucidate the complex dynamics of relaxation and recombination of excitons in TMD MLs [53]. In general, the exciton lifetime τ, measured in time-resolved luminescence dynamics, depends on both radiative and non-radiative (NR) recombination channels with $1/\tau = 1/\tau_{rad} + 1/\tau_{nr}$. The radiative decay channel depends on the electrodynamical environment characteristics due to the Purcell effect while the non-radiative one, having no electromagnetic origin is assumed unchanged. Remarkably, the strong variation of the neutral exciton lifetime reported in Fig. 2 demonstrates that the neutral exciton lifetime at low temperatures is limited by the radiative recombination (controlled here by the Purcell effect) with negligible contribution of NR channels. However we did not observe any effect of the environment on the exciton dynamics for lattice temperatures above 80 K (see

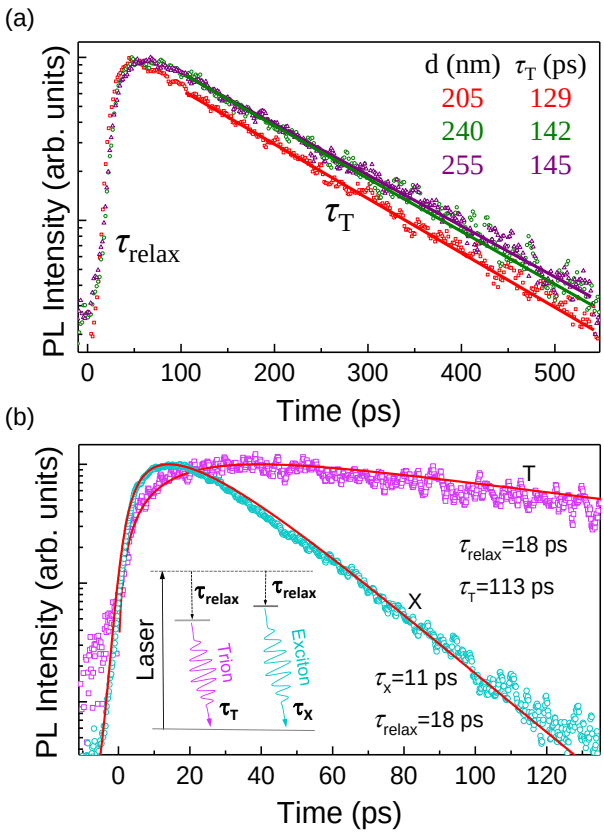

FIG. 3: (a) Normalized photoluminescence intensity of the charged exciton (T) as a function of time for different bottom hBN layer thicknesses d. The full lines correspond to mono-exponential fits of the decay time τ_T. (b) Measured (symbols) and fitted (full line) of neutral (X) and charged (T) exciton dynamics for encapsulated $MoSe_2$ monolayer with a bottom hBN layer thickness $d = 273$ nm (Sample II). Inset: schematics of the two-levels model used to describe both neutral (X) and charged (T) exciton dynamics (see text).

SI [29]). This is due to the fact that the exciton lifetime is no more controlled by purely radiative recombination [54]. The rather small modulation of the trion lifetime observed in Fig. 3 reveals that it is significantly affected by NR recombination. We can infer a NR trion recombination time of the order of $\tau_{nr} \sim 100$ ps, i.e. competitive with the radiative one.

Excellent fits of both the neutral and charged exciton PL dynamics can be obtained with the two-level model using the same relaxation time τ_{relax} from the photogenerated high energy states, inset of Fig. 3(b). As already reported for non-encapsulated TMD MLs [39], we do not find here any evidence of electronic transfer from neutral excitons to trions in $MoSe_2$ ML. This result seems counterintuitive since the PL decay time of the neutral exciton X coincides with the measured PL rise time of the charged exciton, see Fig. 3(b), as if the X lifetime

would be controlled by the trion formation time. This behavior is simply due to the fact that the same energy relaxation time τ_{relax} drives both the neutral exciton PL decay time and charged exciton PL rise time (see SI [29] where also alternative scenarios are discussed).

In conclusion, we have shown that encapsulation of TMD MLs with hBN does not only improve the exciton emission/absorption linewidth by reducing the disorder-induced broadening related to local dielectric fluctuations. The hBN layers surrounding the semiconducting monolayer also have a dramatic impact on the exciton photon coupling through the Purcell effect. We demonstrate that we can control the radiative recombination time by one order of magnitude from ~ 1 ps up to about 10 ps in full agreement with the theoretical analysis. This opens the way to engineer the exciton-photon coupling in these van der Waals heterostructures. An interesting prospect would be to deposit TMD monolayers on top of epsilon-near-zero metamaterials [55] to obtain stronger enhancement of the exciton radiative decay rate.

Acknowledgements. (*) HHF and BH have contributed equally to this work. We thank M. Gurioli, S. Berciaud and A. Poddubny for stimulating discussions. We acknowledge funding from ANR 2D-vdW-Spin, ANR VallEx, ANR MagicValley, Labex NEXT projects VWspin and MILO, ITN Spin-NANO No 676108 and ITN 4PHOTON Nr. 721394. M.A.S. and M.M.G. acknowledge partial support from LIA ILNACS through the RFBR project 17-52-16020. M.A.S. also acknowledges partial support of the Government of the Russian Federation (Project No. 14.W03.31.0011 at the Ioffe Institute). Growth of hexagonal boron nitride crystals was supported by the Elemental Strategy Initiative conducted by MEXT, Japan, and CREST (JP- MJCR15F3), JST. X.M. also acknowledges the Institut Universitaire de France.

[1] E. Purcell, Phys. Rev. **69**, 681 (1946).
[2] D. Kleppner, Rhys. Rev. Lett. **47**, 233 (1981).
[3] W. Jhe, A. Anderson, E. Hinds, D. Meschede, L. Moi, and S. Haroche, Phys. Rev. Lett. **58**, 666 (1987).
[4] H. Benisty, H. De Neve, and C. Weisbuch, IEEE Journal of quantum electronics **34**, 1612 (1998).
[5] J. Gérard, B. Sermage, B. Gayral, B. Legrand, E. Costard, and V. Thierry-Mieg, Phys. Rev. Lett. **81**, 1110 (1998).
[6] M. Bayer, T. Reinecke, F. Weidner, A. Larionov, A. McDonald, and A. Forchel, Phys. Rev. Lett. **86**, 3168 (2001).
[7] F. Cadiz, E. Courtade, C. Robert, G. Wang, Y. Shen, H. Cai, T. Taniguchi, K. Watanabe, H. Carrere, D. Lagarde, et al., Phys. Rev. X **7**, 021026 (2017).
[8] G. Scuri, Y. Zhou, A. A. High, D. S. Wild, C. Shu, K. De Greve, L. A. Jauregui, T. Taniguchi, K. Watanabe, P. Kim, et al., Phys. Rev. Lett. **120**, 037402 (2018).
[9] P. Back, S. Zeytinoglu, A. Ijaz, M. Kroner, and A. Imamoğlu, Phys. Rev. Lett. **120**, 037401 (2018).
[10] K. F. Mak, K. He, Changgu, G. H. Lee, J. Hone, T. F. Heinz, and J. Shan, Nat. Mater. **12**, 207 (2013).
[11] K.-D. Park, T. Jiang, G. Clark, X. Xu, and M. B. Raschke, Nat. Nano. **13**, 59 (2018).
[12] G. Wang, C. Robert, M. Glazov, F. Cadiz, E. Courtade, T. Amand, D. Lagarde, T. Taniguchi, K. Watanabe, B. Urbaszek, et al., Phys. Rev. Lett. **119**, 047401 (2017).
[13] M. Selig, G. Berghäuser, A. Raja, P. Nagler, C. Schüller, T. F. Heinz, T. Korn, A. Chernikov, E. Malic, and A. Knorr, Nat. Communs. **7**, 13279 (2016).
[14] T. Smoleński, M. Goryca, M. Koperski, C. Faugeras, T. Kazimierczuk, A. Bogucki, K. Nogajewski, P. Kossacki, and M. Potemski, Phys. Rev. X **6**, 021024 (2016).
[15] H. Dery, Phys. Rev. B **94**, 075421 (2016).
[16] P. Dey, L. Yang, C. Robert, G. Wang, B. Urbaszek, X. Marie, and S. Crooker, Phys. Rev. Lett. **119**, 137401 (2017).
[17] X. Hong, J. Kim, S.-F. Shi, Y. Zhang, C. Jin, Y. Sun, S. Tongay, J. Wu, Y. Zhang, and F. Wang, Nat. Nano. **9**, 682 (2014).
[18] F. Koppens, T. Mueller, P. Avouris, A. Ferrari, M. Vitiello, and M. Polini, Nat. Nano. **9**, 780 (2014).
[19] T. Galfsky, Z. Sun, C. R. Considine, C.-T. Chou, W.-C. Ko, Y.-H. Lee, E. E. Narimanov, and V. M. Menon, Nano letters **16**, 4940 (2016).
[20] Y.-C. Lee, Y.-C. Tseng, and H.-L. Chen, ACS Photonics **4**, 93 (2016).
[21] Y.-C. Chang, S.-Y. Shiau, and M. Combescot, Physical Review B **98**, 235203 (2018).
[22] G. Wang, A. Chernikov, M. M. Glazov, T. F. Heinz, X. Marie, T. Amand, and B. Urbaszek, Rev. Mod. Phys. **90**, 021001 (2018).
[23] A. V. Stier, N. P. Wilson, K. A. Velizhanin, J. Kono, X. Xu, and S. A. Crooker, Phys. Rev. Lett. **120**, 057405 (2018).
[24] C. Robert, M. Semina, F. Cadiz, M. Manca, E. Courtade, T. Taniguchi, K. Watanabe, H. Cai, S. Tongay, B. Lassagne, et al., Phys. Rev. Materials **2**, 011001 (2018).
[25] C. Schneider, M. M. Glazov, T. Korn, S. Höfling, and B. Urbaszek, Nat. Communs. **9**, 2695 (2018).
[26] K. Tanaka, T. Nakamura, W. Takamatsu, M. Yamanishi, Y. Lee, and T. Ishihara, Phys. Rev. Lett. **74**, 3380 (1995).
[27] I. Abram, I. Robert, and R. Kuszelewicz, IEEE Journal of quantum electronics **34**, 71 (1998).
[28] A. Castellanos-Gomez, M. Buscema, R. Molenaar, V. Singh, L. Janssen, H. S. Van Der Zant, and G. A. Steele, 2D Materials **1**, 011002 (2014).
[29] See Supplementary Material for additional experimental data and theory of spontaneous emission in van der Waals heterostructures which includes Refs. [30–36].
[30] L. Landau and E. Lifshitz. *Statistical Physics, Part 1.* Butterworth-Heinemann, Oxford, 2000.
[31] M. M. Glazov, T. Amand, X. Marie, D. Lagarde, L. Bouet, and B. Urbaszek, Phys. Rev. B, **89** 201302 (2014).
[32] D. Christiansen, M. Selig, G. Berghäuser, R. Schmidt, I. Niehues, R. Schneider, A. Arora, S. M. de Vasconcellos, R. Bratschitsch, E. Malic, and A. Knorr, Phys. Rev. Lett. **119**, 187402 (2017).
[33] S. Shree, M. Semina, C. Robert, B. Han, T. Amand, A. Balocchi, M. Manca, E. Courtade, X. Marie, T. Taniguchi, K. Watanabe, M. M. Glazov, and B. Ur-

baszek, Phys. Rev. B **98**, 035302 (2018).
[34] R. R. Chance, A. Prock, and R. Silbey. In *Advances in Chemical Physics*, pages 1–65. John Wiley & Sons, 1978.
[35] M. M. Glazov, E. L. Ivchenko, A. N. Poddubny, and G. Khitrova, Phys. Solid. State, **53**, 1753 (2011).
[36] F. De Martini, M. Marrocco, P. Mataloni, L. Crescentini, and R. Loudon, Phys. Rev. A **43**, 2480 (1991).
[37] S.-Y. Lee, T.-Y. Jeong, S. Jung, and K.-J. Yee, physica status solidi (b) p. 1800417 (2018).
[38] D. Lagarde, L. Bouet, X. Marie, C. R. Zhu, B. L. Liu, T. Amand, P. H. Tan, and B. Urbaszek, Phys. Rev. Lett. **112**, 047401 (2014).
[39] C. Robert, D. Lagarde, F. Cadiz, G. Wang, B. Lassagne, T. Amand, A. Balocchi, P. Renucci, S. Tongay, B. Urbaszek, et al., Phys. Rev. B **93**, 205423 (2016).
[40] A. Chernikov, C. Ruppert, H. M. Hill, A. F. Rigosi, and T. F. Heinz, Nat. Photon. **9**, 466 (2015).
[41] Z. Wang, L. Zhao, K. F. Mak, and J. Shan, Nano Lett. **17**, 740 (2017).
[42] C. Jin, J. Kim, J. Suh, Z. Shi, B. Chen, X. Fan, M. Kam, K. Watanabe, T. Taniguchi, S. Tongay, et al., Nat. Phys. **13**, 127 (2017).
[43] T. Korn, S. Heydrich, M. Hirmer, J. Schmutzler, and C. Schüller, Appl. Phys. Lett. **99**, 102109 (2011).
[44] E. L. Ivchenko, *Optical spectroscopy of semiconductor nanostructures* (Alpha Science, Harrow UK, 2005).
[45] G. Bourdon, I. Robert, R. Adams, K. Nelep, I. Sagnes, J. Moison, and I. Abram, Appl. Phys. Lett. **77**, 1345 (2000).
[46] E. W. Martin, J. Horng, H. G. Ruth, E. Paik, M.-H. Wentzel, H. Deng, and S. T. Cundiff, arXiv preprint arXiv:1810.09834 (2018).
[47] G. Moody, C. K. Dass, K. Hao, C.-H. Chen, L.-J. Li, A. Singh, K. Tran, G. Clark, X. Xu, G. Berghäuser, et al., Nat. Communs. **6**, 8315 (2015).
[48] T. Jakubczyk, V. Delmonte, M. Koperski, K. Nogajewski, C. Faugeras, W. Langbein, M. Potemski, and J. Kasprzak, Nano Lett. **16**, 5333 (2016).
[49] Y. Zhou, G. Scuri, J. Sung, R. J. Gelly, D. S. Wild, K. De Greve, A. Y. Joe, T. Taniguchi, K. Watanabe, P. Kim, et al., arXiv preprint arXiv:1901.08500 (2019).
[50] C. Rogers, D. Gray Jr, N. Bogdanowicz, T. Taniguchi, K. Watanabe, and H. Mabuchi, arXiv preprint arXiv:1902.05036 (2019).
[51] M. Palummo, M. Bernardi, and J. C. Grossman, Nano letters **15**, 2794 (2015).
[52] G. Wang, L. Bouet, D. Lagarde, M. Vidal, A. Balocchi, T. Amand, X. Marie, and B. Urbaszek, Phys. Rev. B **90**, 075413 (2014).
[53] S. Brem, M. Selig, G. Berghaeuser, and E. Malic, Scientific reports **8**, 8238 (2018).
[54] M. Selig, G. Berghäuser, A. Raja, P. Nagler, C. Schüller, T. F. Heinz, T. Korn, A. Chernikov, E. Malic, and A. Knorr, Nat. Communs. **7**, 13279 (2016).
[55] R. Maas, J. Parsons, N. Engheta, and A. Polman, Nat. Photon. **7**, 907 (2013).